

## Article

# Provincial Land Use and Land Cover Change in Vietnam, 2000–2023: Intensity, Structural Dynamics, and Regional Differentiation

An The Ngo <sup>1,\*</sup>  and Linda See <sup>2,\*</sup> 

<sup>1</sup> Faculty of Natural Resources and Environment, Vietnam National University of Agriculture, Gia Lam, Hanoi 131000, Vietnam

<sup>2</sup> Novel Data Ecosystems for Sustainability (NODES) Research Group, Advancing Systems Analysis Program, International Institute for Applied Systems Analysis (IIASA), Schlossplatz 1, A-2361 Laxenburg, Austria

\* Correspondence: ntan@vnua.edu.vn (A.T.N.); see@iiasa.ac.at (L.S.)

## Abstract

Recent land use and land cover (LULC) transformation in Vietnam raises the question of whether recent changes reflect a uniform national trend or differentiated regional patterns. This study assesses provincial LULC dynamics across 34 provinces using nationally consistent remote-sensing data for 2000, 2020, and 2023. We combine annualized intensity analysis, transition matrices, Shannon entropy, dominant transition analysis, and spatial autocorrelation to compare the magnitude, structure, and spatial organization of LULC change before and after 2020. The results show that annualized land-change rates were substantially higher during 2020–2023 than during 2000–2023, with all provinces showing increased rates of transformation. However, this more recent intensification has not been spatially uniform. Higher increases have been concentrated in southern and delta provinces, while several northern and upland provinces showed lower acceleration. Structural responses also varied across provinces: only four of 34 provinces (11.8%) were classified as both accelerated and structurally concentrated, whereas diversified regimes accounted for about two-thirds of the provinces. Population density was moderately associated with post-2020 magnitude of change but only weakly related to structural configuration, indicating that the magnitude and composition of LULC change represent distinct dimensions. By separating change intensity from structural configuration, this study provides a reproducible framework for identifying differentiated provincial land-change regimes. The results show that recent land cover transformation in Vietnam is not a single national process, but a mosaic of spatially and structurally distinct change patterns.

**Keywords:** land use and land cover change; intensity analysis; structural dynamics; Shannon entropy; spatial autocorrelation; land-change regimes; Vietnam



Academic Editor: Martin Boltziar

Received: 15 April 2026

Revised: 4 June 2026

Accepted: 6 June 2026

Published: 12 June 2026

**Copyright:** © 2026 by the authors.

Licensee MDPI, Basel, Switzerland.

This article is an open access article distributed under the terms and

conditions of the [Creative Commons Attribution \(CC BY\) license](https://creativecommons.org/licenses/by/4.0/).

## 1. Introduction

Land use and land cover change (LULC) represents one of the most visible impacts of global environmental transformation. Over recent decades, rapid urbanization, agricultural intensification, infrastructure expansion, and economic integration have substantially altered land systems across regions [1–3]. These changes not only modify the balance between different land cover types, but they also have implications for greenhouse gas emissions, biodiversity, and ecological processes, as well as socio-economic organi-

zation [4,5]. Understanding both the magnitude and the structural patterns of land cover change is therefore central to land-system science and spatial governance.

Urban areas now contain 45% of the world's population, more than double the share in 1950 [6]. According to the IPCC [7], urban areas expanded by a factor of 2.5 between 1975 and 2015, with most of this growth occurring in Asia and North America. This trend is expected to continue, with projections of 1.2 million km<sup>2</sup> by 2030 [2], while the IPCC [7] projects that urban areas could triple between 2015 and 2050. At the regional scale, numerous studies have examined spatial heterogeneity and the driving forces of land use change, particularly in rapidly transforming Asian regions including the Yangtze River Delta, the Weihe River Basin, coastal Jiangsu, Cambodia, and Guangdong Province [8–12]. These studies have consistently shown that land transformation has been uneven across space and shaped by different combinations of socioeconomic, institutional, topographic, and policy-related factors.

Methodologically, land-change analysis has moved beyond simple area comparisons toward approaches that distinguish the magnitude, structure, and spatial organization of change. Intensity analysis provides a standardized way to compare land-change rates across categories and time intervals, including intervals of unequal duration [13–15]. Entropy-based measures further allow researchers to assess whether transitions are concentrated in a few dominant pathways or distributed across multiple land cover exchanges [16–18]. Spatial autocorrelation methods, including Moran's I and local indicators of spatial association (LISA), complement these approaches by identifying geographic clustering and spatial outliers in land-change processes [19–23].

Despite these advances, many national-scale land cover studies still focus on the magnitude of change, such as total converted area, annual change rates, or class-level gains and losses, while giving less attention to the structural configuration of transition pathways. This is relevant because higher land-conversion rates do not necessarily imply structural simplification. Change may be concentrated in a small number of dominant transitions, or it may diversify across multiple pathways. A framework that explicitly separates change intensity from transition structure and spatial clustering therefore remains useful for comparative land-change analysis.

Vietnam provides a relevant context for applying such a framework. Previous studies have documented rapid urban expansion, agricultural land conversion, and regional land use restructuring, particularly following economic reforms and infrastructure-led development [24–26]. National-scale studies have produced annual LULC change maps and quantified major land cover changes from 1990 or 2000 to 2020, including forest and wetland losses, built-up expansion, and urban and aquaculture growth [27,28]. However, these studies have primarily focused on area change, class-level gains and losses, or broad drivers of built-up expansion, with limited attention to whether provincial land-change dynamics differ in their transition structure or spatial clustering. Regional and provincial studies have provided more localized insights into urban expansion, agricultural land loss, aquaculture development, and peri-urban transformation [29–32], but they do not provide a consistent national comparison of provincial land-change regimes.

To address these methodological gaps in LULC change analysis, a multi-dimensional analytical framework is needed that combines change intensity, structural diversity, dominant transitions, and spatial clustering. By integrating established conversion metrics [14], entropy-based structural measurement [16,17], and spatial autocorrelation analysis [19,20] into a single diagnostic framework, it becomes possible to identify different land-change regimes across units that matter for governance. This would not be possible using only a single indicator approach. In addition, little attention has been given to whether re-

cent land transformation, especially after 2020, reflects a single national trend or different provincial regimes.

Accordingly, this study aims to provide a multidimensional assessment of provincial land cover dynamics in Vietnam, with particular emphasis on post-2020 change, because most previous studies end in 2020. The paper addresses the following three research questions:

1. Has land-conversion intensity continued to accelerate in Vietnam after 2020, and is this acceleration spatially clustered across provinces?
2. How have structural configurations of land transitions evolved, and are acceleration and structural concentration systematically linked?
3. Can provincial land-change regimes be classified based on joint dynamics of intensity and compositional change, and what patterns emerge from such a typology?

By addressing these questions, the study contributes to land-system science in two ways. Empirically, it provides a nationally consistent and province-level comparison of recent land cover change. Conceptually, it develops a regime-based approach that separates the magnitude of change from its structural configuration (or pattern) and combines this with spatial analytical diagnostics within a unified framework. The framework emphasizes comparative characterization of provincial land-change regimes based on observed transition patterns and spatial differentiation. This multidimensional approach goes beyond single-indicator assessments of land change. Instead, it provides a scalable basis for comparing different land governance contexts.

## 2. Materials and Methods

### 2.1. Study Area and Spatial Units

Vietnam is located in mainland Southeast Asia, bordering China to the north and Laos and Cambodia to the west, with an extended eastern coastline along the East Sea. Its elongated north–south configuration and diverse physiographic conditions contribute to substantial regional heterogeneity in LULC patterns and development trajectories (Figure 1). This study covers 34 provinces under Vietnam’s current administrative structure. Provinces have been adopted as the primary scale for analysis because land use planning, land allocation, and regulatory implementation are mainly exercised at this level. In addition, this provides a consistent spatial framework for comparing LULC dynamics across different administrative contexts. Thus, variations in LULC conversion rates, structural configuration, and spatial clustering can be compared across similar levels of territorial governance. All spatial data were harmonized to the current provincial boundaries to ensure comparability across time periods.

### 2.2. LULC Data and Preprocessing

LULC maps for 2000, 2020, and 2023 were obtained from harmonized raster products developed by the Japan Aerospace Exploration Agency (JAXA) [33]. These datasets represent a consistent LULC classification derived from remote sensing. All datasets share identical projection (UTM), spatial resolution (30 m), and grid alignment, ensuring pixel-level comparability across years. Further technical details of the LULC products and preprocessing procedures are provided in the Supplementary Information (S1).

The original JAXA classification scheme was aggregated into six LULC categories to align with the latest Vietnamese national technical regulations [34]: (1) water and wetlands; (2) built-up areas; (3) agriculture; (4) grass and shrubland; (5) forest; and (6) bare and other land.



**Figure 1.** Study area of Vietnam in Southeast Asia and provincial boundaries (34 provinces used as analytical units).

Two temporal intervals were defined for the change analysis:

- Period 1 (P1): 2000–2020 (20 years)
- Period 2 (P2): 2020–2023 (3 years, the most recent data available at the time of analysis).

All rasters were co-registered and clipped to the provincial boundaries. The preprocessing ensured spatial consistency prior to transition matrix construction and structural change analysis.

### 2.3. Transition Matrix and Mass-Balance Accounting

For each province and time interval, a  $6 \times 6$  LULC transition matrix was constructed through raster overlay, with transition areas derived from pixel counts multiplied by cell area. Each element  $T_{ij}$  represents the area converted from category  $i$  at time  $t_1$  to category  $j$  at time  $t_2$ . Here,  $t_1$  and  $t_2$  denote the beginning and ending years of each analysis interval (2000–2020 and 2020–2023), respectively. Diagonal elements ( $T_{ii}$ ) indicate persistence, while off-diagonal elements capture LULC conversions.

The total provincial area is conserved such that the row sums equal the LULC areas at  $t_1$  and column sums equal areas at  $t_2$ , ensuring mass-balance consistency:

$$\sum_j T_{ij} = A_i^{(t_1)}, \sum_i T_{ij} = A_j^{(t_2)}, \quad (1)$$

This matrix-based accounting follows the land-change analytical framework of Pontius et al. [13] and provides the basis for subsequent structural and entropy-based indicators. In addition to the provincial matrices, an aggregated Vietnam-wide transition matrix was constructed for each interval by summing transition areas across all provinces. This national matrix (Supplementary Information, S4) was used to derive area-weighted national benchmark values for comparison with provincial transition structures and change intensities.

#### 2.4. Intensity Analysis

Intensity analysis was employed to compare land-change magnitude across provinces and unequal time intervals following the framework of Aldwaik and Pontius [14]. The method standardizes change relative to total area and interval duration, enabling consistent cross-period comparison. Because the analysis is based on transitions between LULC maps for 2000, 2020, and 2023, the calculated intensities represent annualized average rates within each interval rather than year-by-year observations.

At the interval level, the annualized change intensity  $S$  was calculated as:

$$S = \frac{C}{A \times \Delta t}, \quad (2)$$

where  $C$  denotes the total converted area (sum of all off-diagonal transition matrix elements),  $A$  is the total provincial area, and  $\Delta t$  is the interval duration in years. The same formulation was also applied to the aggregated Vietnam-wide transition matrix to calculate national annualized change intensity for each period. To evaluate the post-2020 acceleration, the change in intensity was defined as:

$$\Delta S = S_{P2} - S_{P1}, \quad (3)$$

This formulation ensures comparability between the 20-year period (P1: 2000–2020) and the 3-year period (P2: 2020–2023). Given the sample size ( $n = 34$ ), the paired  $t$ -test is considered robust for comparative purposes.

At the category level, the total loss from category  $i$  and the total gain to category  $j$  was derived from the transition matrix as:

$$L_i = \sum_{j \neq i} T_{ij}, G_j = \sum_{i \neq j} T_{ij}, \quad (4)$$

The category-specific annual intensities were then calculated as:

$$I_i^{loss} = \frac{L_i}{A \times \Delta t}, I_j^{gain} = \frac{G_j}{A \times \Delta t} \quad (5)$$

These categories were classified as active or dormant by comparing their gain or loss intensities with the overall interval intensity  $S$ , thereby identifying LULC types that changed disproportionately relative to the provincial average. The aggregated national transition matrix was additionally used to identify dominant national transition pathways and provide a benchmark for interpreting provincial deviations from the country-wide land-change pattern.

#### 2.5. Spatial Autocorrelation of Acceleration

The spatial dependence in the post-2020 intensity change ( $\Delta S$ ) was evaluated using global and local spatial autocorrelation statistics. A first-order queen contiguity spatial weights matrix was constructed to define provincial neighborhood relationships, such that two provinces were considered neighbors if they shared either a common border or a vertex. The matrix was row-standardized prior to the analysis to ensure comparability across provinces with different numbers of neighbors.

The global spatial autocorrelation was assessed using Moran's  $I$  [19]:

$$I = \frac{n}{S_0} \frac{\sum_i \sum_j w_{ij} (x_i - \bar{x})(x_j - \bar{x})}{\sum_i (x_i - \bar{x})^2}, \quad (6)$$

where  $n = 34$  provinces;  $x_i$  represents  $\Delta S$  in province  $i$ ;  $\hat{x}$  is the mean  $\Delta S$ ;  $w_{ij}$  denotes the row-standardized spatial weights; and  $S_0 = \sum_i \sum_j w_{ij} x_j$ . Under the null hypothesis of spatial randomness, the expected value is  $E[I] = -1/(n-1)$ . The statistical significance was evaluated using 999 random permutations with a two-tailed  $\alpha = 0.05$ .

The local spatial patterns were examined using Local Moran's I [20], defined as:

$$I_i = z_i \sum_j w_{ij} z_j \quad (7)$$

where  $z_i = (x_i - \hat{x})/s$  is the standardized  $\Delta S$  value and  $s$  is the standard deviation across provinces. The sign of  $z_i$  and its spatial lag  $\sum_j w_{ij} z_j$  determines the cluster typology. The provinces were classified as High–High (above-average  $\Delta S$  surrounded by above-average neighbors), Low–Low (below-average  $\Delta S$  surrounded by below-average neighbors), High–Low, or Low–High spatial outliers. The significance was determined using 999 permutations (pseudo- $p < 0.05$ ), while non-significant provinces were interpreted as exhibiting no detectable local spatial autocorrelation.

This framework shows how acceleration patterns at the provincial level relate to wider spatial differences, while staying consistent with the intensity-based indicators described above.

### 2.6. Structural Concentration of LULC Change

To evaluate compositional restructuring beyond change magnitude, Shannon entropy was applied to the distribution of inter-category transition shares [16]. While intensity analysis captures how much land changes, entropy was used to quantify the distribution of inter-category land cover transitions within each province and period. Thus, entropy represents one component of a broader diagnostic framework rather than a standalone measure of land-system complexity.

For each province and interval, transition shares were calculated from the off-diagonal elements of the transition matrix:

$$p_{ij} = \frac{T_{ij}}{C}, i \neq j, \quad (8)$$

where  $T_{ij}$  denotes the area converted from category  $i$  to category  $j$ , and  $C$  is the total converted area (sum of all  $T_{ij}$  with  $i \neq j$ ). The persistence terms  $T_{ij}$  were excluded to ensure comparability across provinces regardless of the total unchanged area.

The Shannon entropy was then computed as:

$$H = -\sum_{i \neq j} p_{ij} \ln(p_{ij}) \quad (9)$$

Higher values of  $H$  indicate a more diversified transition structure (change distributed across multiple categories), whereas lower values indicate concentration in fewer dominant transitions. The structural reorganization between periods was assessed as:

$$\Delta H = H_{P2} - H_{P1} \quad (10)$$

Negative values of  $\Delta H$  indicate increasing structural concentration, while positive values reflect diversification of LULC transitions. The entropy values are interpreted relative to the distribution of transition shares within each province and period.

### 2.7. Governance Typology

To synthesize the acceleration and structural reorganization into an interpretable framework, the provinces were classified along two dimensions: (i) the acceleration of change intensity ( $\Delta S$ ) and (ii) the structural concentration of the transitions ( $\Delta H$ ).

The acceleration of reorganization was evaluated relative to the provincial distribution of  $\Delta S$ . Provinces with  $\Delta S$  exceeding the median were classified as accelerated, while those at or below the median were considered stable. This threshold ensures balanced group sizes and provides a data-driven classification based on the observed distribution.

Structural configuration was determined through entropy change analysis ( $\Delta H$ ). Provinces were classified as concentrated when  $\Delta H \leq -0.10$ , diversified when  $\Delta H \geq 0.10$ , and structurally stable when  $-0.10 < \Delta H < 0.10$ . The  $\pm 0.10$  threshold was adopted as a practical and interpretable criterion to distinguish noticeable structural reorganization from minor fluctuations near zero. The selected thresholds were intended to support exploratory comparison of provincial land-change patterns rather than to define fixed universal categories.

This choice is consistent with the context-dependent application of entropy-based thresholds in land-change analysis, where no universal cutoff exists and threshold selection depends on analytical objectives and data characteristics [35]. A formal sensitivity analysis using alternative entropy thresholds ( $-0.05$  and  $-0.15$ ) was conducted, and the results are reported in Supplementary Material S8. However, some provinces near classification boundaries showed minor changes in category assignment. Structurally stable cases were consolidated with diversified regimes to maintain analytical parsimony and policy relevance.

The cross-classification of these two dimensions yielded four governance-relevant regime types: Accelerated–Concentrated (A–C), Accelerated–Diversified (A–D), Stable–Concentrated (S–C), and Stable–Diversified (S–D). This typology serves as a diagnostic framework for interpreting spatial variation in governance implications.

### 2.8. Population Density and Land-Change Coupling

Population density in 2023 was incorporated as a proxy for urbanization pressure to examine its association with post-2020 land-change dynamics. The variable was included to support contextual interpretation of provincial land-change patterns, not to establish causal relationships or quantify the relative contribution of underlying drivers. A two-tailed Pearson correlation analysis was used to assess the linear relationships between population density and (i) post-2020 change intensity ( $S_{P2}$ ), (ii) post-2020 entropy ( $H_{P2}$ ), and (iii) structural reorganization between periods ( $\Delta H$ ).

To explore potential institutional differentiation, the provinces were additionally grouped by administrative status (“municipal city” versus “province”). Comparative analysis was then conducted using independent-sample Mann–Whitney tests to evaluate differences in the rates of transformation and structural configuration. This complementary assessment provides contextual interpretation of demographic and governance influences on observed land-change regimes without implying causal attribution.

## 3. Results and Discussion

### 3.1. Post-2020 Increase in LULC Change Intensity and Spatial Clustering

The annual LULC change intensity ( $S$ ) was markedly higher during the 2020–2023 interval across the 34 provinces. The values reported here represent provincial annual intensities, while a separate national benchmark was derived from the aggregated Vietnam-wide transition matrix for comparison. Mean values rose from 1.47% per year during 2000–2020 (P1) to 11.37% per year during 2020–2023 (P2) (Table 1), yielding a mean increase

( $\Delta S$ ) of +9.89 percentage points. All provinces exhibited positive  $\Delta S$  values. Notably, the maximum annualized rate of change recorded during P1 (2.55%) remains below the minimum observed during P2 (5.91%), with no overlap between the two distributions. A paired-sample *t*-test confirms that the post-2020 increase is highly significant ( $p < 0.001$ ; see Supplementary Information, S6).

**Table 1.** The provincial annual LULC change intensity (*S*) and aggregated national summary statistics before and after 2020 ( $n = 34$ ).

Indicator	2000–2020	2020–2023
Mean <i>S</i> (%/year)	1.47	11.37
Standard deviation	0.47	3.22
Minimum	0.75	5.91
Maximum	2.55	20.41
National benchmark <i>S</i> (%/year)	1.83	9.94

At the national level, annualized land-change rates also increased substantially, from 1.83% during P1 to 9.94% during P2. This national benchmark provides a reference for interpreting how individual provinces differ from the overall country-wide land-change pattern.

This distributional separation is illustrated in Figure 2 where the boxplot for P2 is entirely above P1. Moreover, the amount of dispersion has expanded substantially (SD increasing from 0.47 to 3.22), which indicates an intensified interprovincial differentiation under the higher-intensity regime. Although the national benchmark indicates an overall acceleration after 2020, the wide provincial dispersion demonstrates that the magnitude of land-change conversion remained highly uneven across provinces. Comparable stepwise accelerations have been documented in rapidly urbanizing regions of East and Southeast Asia, where infrastructure expansion and economic restructuring have triggered nonlinear land dynamics [2,8]; this reinforces the finding that the observed shift reflects a broader regional pattern of accelerated land transformation.

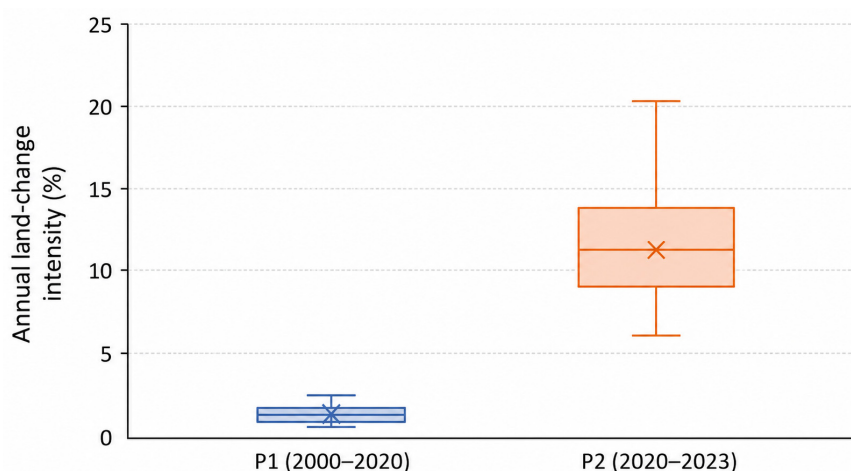


**Figure 2.** The distribution of provincial annual land-change intensity across the two periods (P1: 2000–2020; P2: 2020–2023).

All LULC categories exhibited intensified changes during P2 (Figure 3), with agricultural land showing the most pronounced decline, particularly after 2020. In contrast, forest and shrubland expanded substantially, indicating a redistribution of land among major classes, instead of uniform growth across all categories. These patterns highlight the compositional dimension of land change at the class level, complementing the intensity-based

assessment presented above. Supporting class-level statistics are further detailed in the conversion matrices (Supplementary Information, S4), which quantify the inter-category flows underlying these net changes.

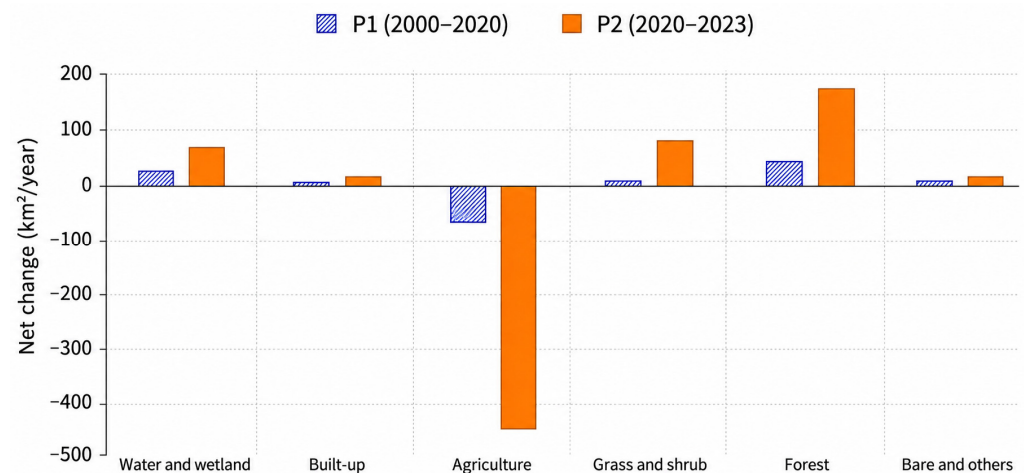


**Figure 3.** Annual net change in LULC categories during P1 (2000–2020) and P2 (2020–2023).

At the national level, agricultural land accounted for the largest share of total converted area in both periods, contributing 68.9% of gross losses during P1 and 72.4% during P2. The dominant national transition pathway shifted from agriculture-to-water/wetland conversion during 2000–2020 (1003.46 km<sup>2</sup>) to agriculture-to-forest conversion during 2020–2023 (828.05 km<sup>2</sup>). This comparison further highlights that many provinces diverged from the aggregated national transition pattern, reinforcing the spatial heterogeneity of post-2020 land-change processes.

The spatial distribution of provincial change intensity differences ( $\Delta S = S_{P2} - S_{P1}$ ) reveals clear regional contrasts (Figure 4). Higher values are concentrated in southern and delta provinces, whereas northern mountainous provinces generally exhibit lower, although still positive values. The absence of negative values indicates that increases in the rate of annualized change are observed across all provinces. This pattern shows a widespread rise in land-change intensity, with substantial variation in magnitude across space.

The Global Moran's I for  $\Delta S$  indicates significant positive spatial autocorrelation ( $I = 0.492$ ;  $z = 4.06$ ;  $p < 0.001$ ), confirming the clustering of provinces with similar rates of change. Such spatial dependence is commonly observed in land-change studies [20,36]. The magnitude of Moran's I observed here is comparable to values reported for spatially clustered urban expansion in eastern China [8].

The Local Moran's I (999 permutations, Queen contiguity,  $p < 0.05$ ; see Supplementary Information, S7) identified six statistically significant High–High provinces forming a southern hotspot of accelerated change. In contrast, Cao Bang and Hue province were classified as Low–Low clusters, embedded within zones of comparatively weaker acceleration (Figure 5). No significant High–Low or Low–High outliers were detected. These findings suggest broader regional patterns of acceleration, not just isolated anomalies in specific administrative areas.

The spatial clustering found here matches broader evidence that LULC change often spreads across regions through processes shaped by economic integration and governance capacity [37]. Provinces in metropolitan corridors and delta areas tend to change faster in a coordinated way. In contrast, remote upland regions usually show slower and weaker change. These differences may reflect variation in infrastructure connectivity, regional development trajectories, and institutional capacity, which have been widely associated

with uneven LULC change across space [38], but the present analysis does not formally test these explanatory mechanisms.

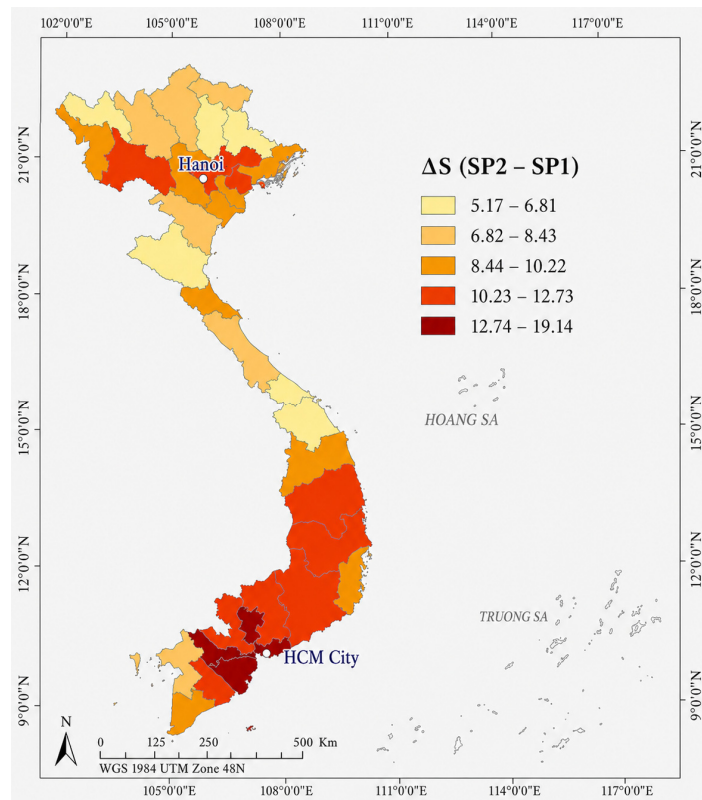


**Figure 4.** Spatial distribution of the increase in the land-change intensity ( $\Delta S = S_{P2} - S_{P1}$ ).

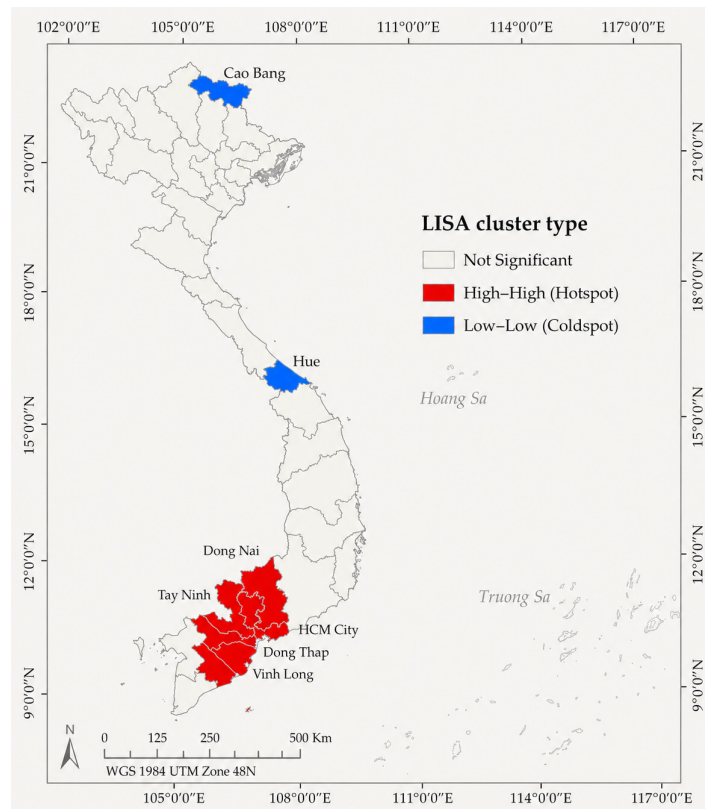


**Figure 5.** Spatial clusters of provincial increases in land-change intensity ( $\Delta S$ ) during 2020–2023 based on Local Moran’s I (LISA).

Collectively, the statistical separation between P1 and P2, the universal positive acceleration, the increased dispersion, and the emergence of spatial clustering provide robust evidence that the post-2020 period represents a distinct and spatially organized period of elevated annual transformation. Note that these spatial clusters should be interpreted as indicators of geographic organization rather than evidence of causality. The LISA results show where provinces with similar increases in annualized change intensity are spatially grouped, but they do not identify the processes responsible for those groupings. The clusters therefore provide a basis for formulating hypotheses about regional development corridors, infrastructure connectivity, or shared governance conditions, which would need to be tested through additional explanatory modeling. The next section examines whether this intensified change is concentrated in a small number of dominant transitions or distributed across multiple pathways.

### 3.2. Structural Differentiation of LULC Transition Regimes

While Section 3.1 demonstrated that LULC change intensity increased markedly after 2020, the magnitude alone does not reveal whether provincial land systems became structurally simplified or diversified. To assess compositional restructuring, the Shannon entropy ( $H$ ) of the transition shares and its temporal change ( $\Delta H = H_{P2} - H_{P1}$ ) were examined across all provinces.

At the aggregate level, measured as the mean across provinces, entropy increased from 2.399 in 2000–2020 (P1) to 2.522 in 2020–2023 (P2). This suggests that transition portfolios did not simplify during this period. Yet this average increase obscures considerable divergence across provinces. For example, seven provinces (20.6%) experienced structural concentration ( $\Delta H \leq -0.10$ ), ten provinces (29.4%) remained structurally stable ( $-0.10 < \Delta H < 0.10$ ), and seventeen provinces (50.0%) exhibited diversification ( $\Delta H \geq 0.10$ ). Two provinces showed strong concentration ( $\Delta H \leq -0.30$ ), whereas six displayed strong diversification ( $\Delta H \geq 0.30$ ). This variation in  $\Delta H$  values indicates that post-2020 changes in intensity did not consistently result in structural simplification.

Figure 6 illustrates three broad spatial tendencies. First, structural concentration is primarily observed in several northern interior provinces. In these cases, higher annualized change rates coincide with an increasing dominance in a limited set of transitions, indicating concentration in a small number of transition pathways. Similar concentration patterns, where land-change dynamics are dominated by a limited set of transitions, have been reported in frontier or resource-oriented regions [17,37].

Second, pronounced diversification occurs in several highly urbanized and industrialized provinces. Here, higher annualized change rates were accompanied by expansion in the effective number of transition types, indicating structural broadening. Comparable diversification patterns (characterized by multiple concurrent transition pathways) have been observed in rapidly urbanizing regions such as eastern China [8,36].

Third, parts of the southern region exhibited mixed responses. Although Section 3.1 identified a High–High intensity hotspot in the south, several provinces within this cluster showed limited or negative entropy change. This pattern indicates that increased annualized change rates in these provinces have largely amplified pre-existing dominant pathways without substantial reorganization of transition composition. Similar patterns, where increasing magnitudes of change reinforce dominant transitions without diversification, have been reported in intensifying agricultural systems [38].

Importantly, change intensity and structural restructuring were only weakly associated. The Pearson correlation between  $\Delta S$  and  $\Delta H$  is  $-0.173$  ( $n = 34$ ), indicating no systematic coupling between magnitude and compositional change. This weak association, where

increases in land-change magnitude do not necessarily correspond to diversification or concentration, has also been observed in previous land-change studies [1,37].

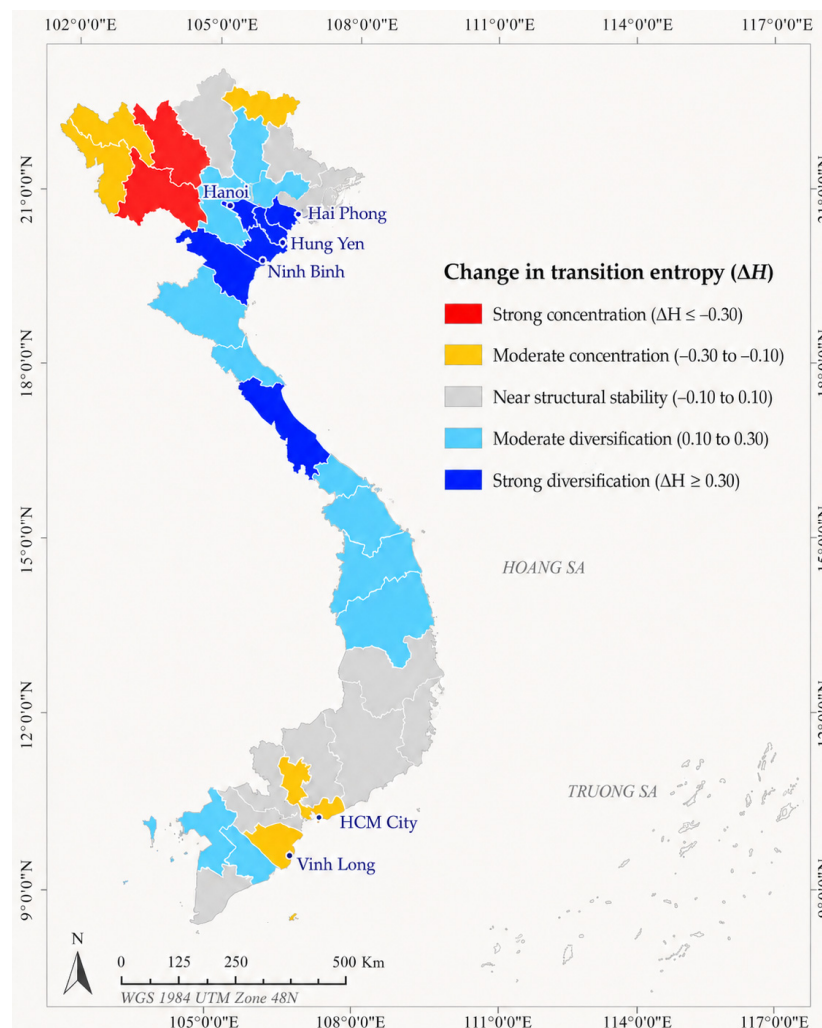


**Figure 6.** Provincial variation in structural change in transition composition ( $\Delta H = H_{P2} - H_{P1}$ ) during 2020–2023.

From a land-system perspective, lower entropy means that change is becoming concentrated in fewer pathways, indicating stronger structural dependence, while higher entropy indicates a wider range of transition pathways. Entropy-based approaches have been widely used to distinguish between concentrated and diversified land-change structures under socio-economic transitions [17].

Overall, the entropy analysis shows that the post-2020 period has been defined not only by higher annualized change rates, but also by different structural trajectories across space. Provinces showed three main patterns: (i) simplifying high-intensity change, (ii) diversifying high-intensity change, and (iii) a stronger intensity with little compositional change. These findings suggest that the amount of land change and the structure of that change should be treated as separate dimensions. The next section examines whether structural concentration is linked to the dominance of specific transition pathways.

### 3.3. Dominant Transition Pathways Under the Accelerated Regime (2020–2023)

Building on the measured intensity and structural patterns, this section examines dominant transition pathways to clarify the compositional drivers of post-2020 LULC change. For the 2020–2023 period (P2), the transition contributing the largest share of

total converted area within each province was identified as the maximum transition share (*MaxR*). Specifically, *MaxR* corresponds to the inter-category transition  $T_{ij}$  with the highest proportion  $p_{ij} = T_{ij}/C$ , where  $C$  is the total converted area of the province during P2.

Across 34 provinces, the dominant transition accounted on average for 25.7% of total LULC change ( $SD = 9.8\%$ ), ranging from 12.9% to 57.9% (Figure 7). This shows that pathway concentration varies greatly across provinces. Provinces with larger dominant shares also tended to show declining entropy (Section 3.2), indicating that structural concentration is associated with greater dependence on a limited number of transition flows [17].

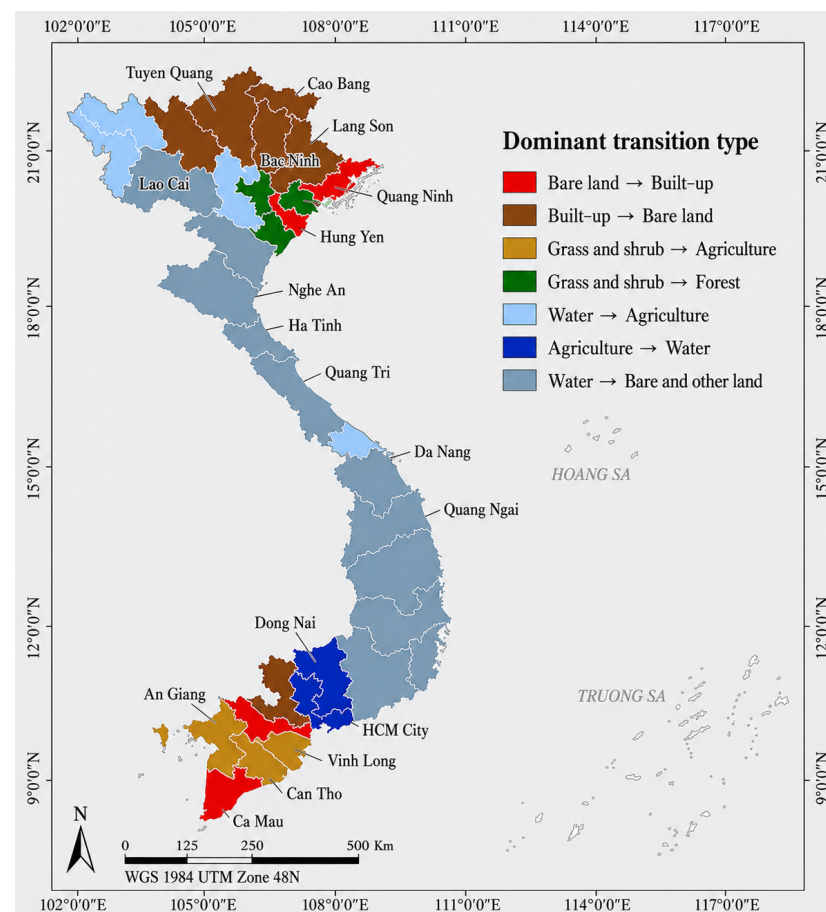


**Figure 7.** Dominant provincial LULC transition pathway by province during 2020–2023, classified by the transition contributing the largest share (*MaxR*) of total LULC change intensity.

Several dominant pathways recurred across a large proportion of provinces. In particular, Water → Bare and other land, Built-up → Bare and other land, and Bare and other land → Built-up are the most frequently observed dominant transitions, accounting for more than half of all provinces. This indicates that post-2020 LULC change was shaped by a limited set of recurring transition types at the provincial level. The recurrence of these pathways across multiple provinces suggests that recent land-change dynamics have been associated with broader regional development processes, including urban expansion, land reallocation, and changing land–water interactions.

While the dominant transition map highlights the most influential pathway in each province, the conversion matrices provide complementary evidence on the overall structure of land reallocation. At the national level, large-volume transitions during P2 were strongly associated with Agricultural land, particularly exchanges between Agriculture, Forest, and Water (Supplementary Information, S4). This contrast indicates that dominant provincial pathways do not necessarily correspond to the largest aggregate flows, but instead, they

reflect the most locally influential transitions within each province, which become evident in the spatial patterns discussed below.

In several northern provinces, dominant transitions occurred between Bare and other land and Built-up surfaces. Such bidirectional patterns, where both Bare and other land  $\rightarrow$  Built-up and Built-up  $\rightarrow$  Bare and other land transitions are prominent, have been reported in rapidly urbanizing regions of East Asia [2,8]. The presence of both directions suggests iterative land reallocation processes within provinces.

By contrast, a contiguous belt of central provinces is characterized by Water  $\rightarrow$  Bare and other land transitions. Similar land–water boundary transitions have been documented in regions undergoing intensive land–water reconfiguration [24,37]. The consistent occurrence of this pathway across provinces indicates regionally coherent transformation patterns.

In southern delta provinces, the main transitions often occurred within Agricultural exchanges, such as Agriculture  $\rightarrow$  Water and Grass/Shrub  $\rightarrow$  Agriculture. Comparable agricultural transition patterns, particularly exchanges between agriculture and water-related uses, have been observed in Southeast Asian lowland systems [4]. These patterns indicate shifts in dominant land use exchanges within agricultural systems.

Statistically, provinces classified as structurally concentrated ( $\Delta H \leq -0.10$ ) exhibited significantly higher dominant shares (mean = 35.4%) than diversified provinces ( $\Delta H \geq 0.10$ ; mean = 22.1%;  $p < 0.05$ ). This result confirms that declining entropy is linked to stronger dominance by certain pathways. However, the dominant share is not strongly correlated with the magnitude of acceleration, reinforcing the earlier finding that intensity and structural configuration are partly independent dimensions of land-change regimes [1].

Overall, the post-2020 period is not explained by a single nationwide transition mechanism. Instead, Vietnam has shown regionally differentiated dominant pathways, including construction-related exchanges in the north, hydrological adjustments in the central provinces, and agricultural restructuring in the south. This heterogeneity (reflected in different dominant transition types across regions) is consistent with findings that land-change patterns vary across regional land systems [36,37]. Identifying dominant transitions therefore complements the intensity and entropy metrics by showing how changes in the rates of transformation are expressed through specific LULC exchanges.

### 3.4. Demographic Pressure and Regime Configuration

Sections 3.1–3.3 show that post-2020 LULC change in Vietnam has been characterized by faster change intensity, spatial clustering, and differences in dominant transition pathways. An additional question is whether these observed patterns are statistically associated with demographic pressure, represented here by population density as an indicator of demographic concentration and urbanization pressure. More specifically, do provinces with higher population density also show stronger land-change rates and greater structural concentration?

Population density varies widely across the 34 provinces, with a small number of highly urbanized municipalities (“City” units) and a larger group of mainly non-metropolitan provinces. Correlation analysis shows a moderate positive association between population density and post-2020 land-change intensity ( $S_{P2}$ ) (Pearson’s  $r \approx 0.45$ ,  $p < 0.01$ ). This means that provinces with a higher population density generally showed higher annual conversion rates.

This finding is consistent with a large body of land-change literature showing that a higher population concentration is commonly associated with stronger land conversion pressure, especially in rapidly developing regions [2,39]. Greater demographic concentra-

tion is often linked to increased demand for housing, infrastructure, and industrial land, which may contribute to accelerated land transformation.

However, the moderate size of the correlation suggests only a partial, not deterministic, relationship. Population density by itself explains only part of the variation in  $S_{P2}$ . Some provinces with a medium population density still showed rapid acceleration, while some very densely populated municipalities showed only moderate increases. Similar partial decoupling between demographic growth and land-change magnitude has been reported in transitional economies, where institutions and planning systems influence how demographic pressure affects land change [37,38].

In contrast, demographic pressure only has a weak relationship with structural configuration. The correlation between population density and entropy ( $H_{P2}$ ) is small and not statistically significant ( $|r| < 0.20$ ,  $p > 0.10$ ), and it is only weakly related to structural change ( $\Delta H$ ). These results suggest that more densely populated provinces do not consistently have either more concentrated or more diversified transition portfolios.

The lack of a strong relationship between population density and entropy is consistent with broader land-system research showing that compositional restructuring depends less on demographic size and more on institutional, sectoral, and planning contexts [1,36]. Population growth may increase the volume of land conversion, but whether that change becomes more concentrated or more diversified depends on development policies, land allocation systems, and sectoral investment patterns.

Administrative differences also shape these dynamics. Provinces classified as “City” units had significantly higher average  $S_{P2}$  than “Province” units ( $p < 0.05$ ), which is consistent with the concentration of infrastructure expansion and redevelopment in metropolitan areas. However, differences in entropy ( $H_{P2}$ ) and structural change ( $\Delta H$ ) between the two groups are not statistically significant. This suggests that urbanized administrative status increases the magnitude of land change without consistently affecting its structural configuration.

These findings show that the relationship between demography and land-change regimes is uneven. Higher population density can support more intense land conversion, but it does not automatically lead to structural concentration. Whether transition pathways become more concentrated or more diverse seems to depend more on governance arrangements and sectoral strategies than on demographic scale alone.

This partial decoupling also reinforces the point made in Sections 3.2 and 3.3 that magnitude ( $\Delta S$ ) and structural change ( $\Delta H$ ) are different aspects of land-system transformation. As a result, monitoring demographic pressure alone is not enough to predict regime configuration. This distinction provides the empirical basis for the governance-oriented typology developed in Section 3.5.

### 3.5. Governance Typology of Provincial Land-Change Regimes

By combining the distribution of the change intensity ( $\Delta S$ ) and the structural change ( $\Delta H$ ), it is possible to identify different provincial land-change regimes, where provinces are classified into four analytical regime types: Accelerated–Concentrated (A–C), Accelerated–Diversified (A–D), Stable–Concentrated (S–C), and Stable–Diversified (S–D). The classification thresholds have been defined in Section 2.7. The resulting spatial configuration is shown in Figure 8.

As shown in Figure 8, regime types are unevenly distributed across the country. A–D provinces form the largest group (13 of 34; 38.2%), followed by S–D (10 provinces; 29.4%), S–C (seven provinces; 20.6%), and A–C (four provinces; 11.8%). Together, the diversified regimes (A–D + S–D) account for about two-thirds of all provinces, indicating

that structural diversification has been more common than pathway concentration during the 2020–2023 period.

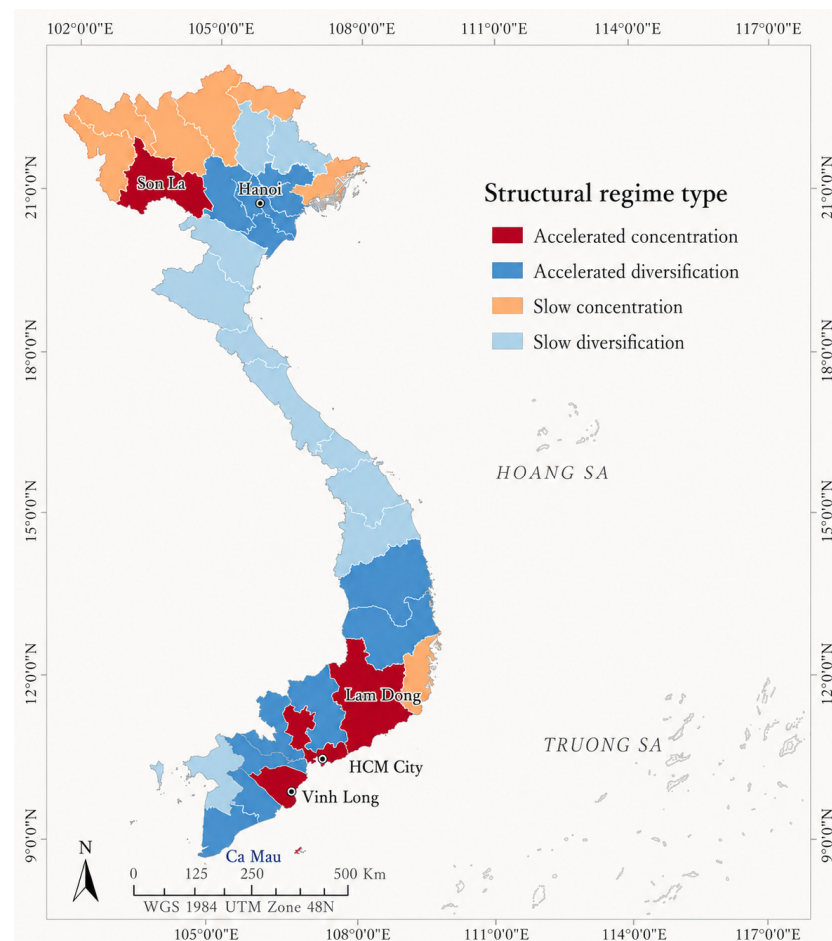


**Figure 8.** Provincial structural regime typology of LULC change during 2020–2023 based on change intensity and transition configuration.

A–C provinces represent the most structurally intensive regime. They combine above-median change intensity with declining entropy, meaning that land conversion is concentrated in a limited number of transition pathways. From a land-system perspective, this pattern indicates increasing dependence on a limited number of pathways and potential sensitivity to pathway-specific dynamics. Concentration patterns dominated by a limited number of transitions have also been reported in rapidly transforming regions [17,37].

A–D provinces show high change intensity, with change distributed across several transition pathways. This pattern indicates restructuring across multiple pathways with no single transition becoming dominant. Diversification patterns involving multiple concurrent transition pathways have been observed in dynamic urban–rural systems [2,5].

S–C provinces show moderate intensity with increasing concentration in a smaller number of pathways. Although their total converted area is lower than in the high-intensity regimes, declining entropy indicates structural specialization. Similar patterns of increasing concentration into fewer transition pathways over time have been reported in specialized or resource-dependent systems [38].

S–D provinces show both moderate intensity and stable or increasing entropy. These provinces reflect comparatively balanced transformations, with no dominant transition emerging. Balanced patterns with multiple coexisting transitions and no clear dominance have been associated with gradually evolving land systems [1].

Spatially, the regime types do not form a simple core–periphery pattern. Instead, high-intensity and stable regimes are distributed across macro-regions, indicating that post-2020 land transformation is not uniformly structured across space.

Importantly, the typology demonstrates that change intensity and structural configuration are distinct dimensions. Only a small number of high-intensity provinces fall into the concentrated category, confirming that higher land-change intensity does not necessarily correspond to simpler transition structures. Conversely, structural concentration can also occur in provinces with only moderate intensity. This multidimensional classification supports land-change research that emphasizes the need to consider both the magnitude and structure of change [1,37].

By combining intensity, entropy dynamics, and spatial configuration, the typology provides a comparative framework for interpreting provincial land-change regimes. Instead of presenting post-2020 land transformation as a uniform national pattern, the results reveal a mosaic of structurally distinct regimes with different transformation characteristics. Section 3.6 discusses the governance implications of these different regimes.

### *3.6. Implications for Differentiated Provincial Land Governance*

The preceding analyses show that LULC change in Vietnam after 2020 is not uniform in terms of change intensity or structural configuration across provinces. Instead, provinces show different regimes shaped by different combinations of intensity ( $\Delta S$ ) and compositional restructuring ( $\Delta H$ ). These results provide a basis for considering differentiated governance approaches, especially for monitoring priorities, regulatory focus, and institutional coordination.

#### *3.6.1. Pathway-Specific Oversight Under Concentrated Acceleration*

Provinces classified as A–C combine high change intensity with declining entropy, meaning that change is concentrated in only a few transition pathways. In these contexts, governance challenges arise not only from the amount of change, but also from growing structural dependence. This concentration means that regulatory oversight may need to focus more closely on dominant transitions, because cumulative impacts can increase when change is concentrated in just a few forms.

Land governance research suggests that this kind of pathway dependence can create lock-in effects, where institutions and investment patterns reinforce particular land use trajectories [37]. This highlights the importance of monitoring dominant transitions and their cumulative effects.

#### *3.6.2. Coordinated Management Under Diversified Acceleration*

A–D provinces show high conversion intensity spread across multiple transition pathways. This pattern reflects multi-sectoral restructuring across several land use categories. In these provinces, governance becomes more complex because urban, agricultural, and infrastructural pressures occur simultaneously.

Research on multi-level and cross-sector land governance highlights the importance of coordination when land systems undergo diversified transformation [1,5]. In such contexts, monitoring approaches that consider both total conversion and its distribution across pathways may be more informative than focusing on a single transition type.

#### *3.6.3. Structural Consolidation Under Moderate Intensity*

S–C provinces show that structural specialization can develop even when overall intensity change remains moderate. These regimes suggest gradual consolidation of LULC orientation. In such contexts, governance attention may shift toward tracking longer-term structural changes in addition to total conversion levels.

Studies of land-system transitions indicate that gradual specialization can increase dependence on specific land use pathways, especially in agriculture- or resource-oriented systems [17]. Assessing structural concentration together with intensity can therefore help identify emerging pathway dependence.

#### 3.6.4. Balanced Adjustment Under Stable–Diversified Regimes

S–D provinces show moderate intensity with relatively balanced transition patterns. This suggests adaptive land transformation that is not highly disruptive. In these contexts, governance may focus on maintaining flexibility in land use monitoring and detecting gradual structural changes.

Land-change research suggests that stability and diversification can be associated with adaptive land systems under socio-economic transition [1]. These patterns indicate the presence of multiple coexisting transitions without a dominant pathway.

#### 3.6.5. Regime-Sensitive Governance as Analytical Contribution

A key conclusion of this study is that the amount of land change and the structure of that change are separate dimensions. Higher annualized rates of change do not necessarily correspond to structural simplification, and structural concentration can also emerge under moderate levels of transformation. Governance frameworks that focus only on total conversion may therefore miss early signs of structural dependence or diversification.

By combining intensity analysis, entropy-based structural assessment, dominant transition analysis, and spatial clustering, the regime typology offers an analytical framework for interpreting provincial land-change patterns in a more differentiated way. Instead of assuming that all provinces need the same regulatory response, the framework supports interpretation that is sensitive to specific regime characteristics. This is in line with wider land-system research that emphasizes the importance of multidimensional approaches to LULC change [1,37].

Overall, Vietnam’s post-2020 land transformation reflects spatially differentiated combinations of change intensity and structural dynamics. Recognizing this heterogeneity is essential for understanding how land governance interacts with spatially varied transformation patterns.

## 4. Limitations

Several limitations and sources of uncertainty should be acknowledged. These relate primarily to data accuracy, entropy interpretation, temporal comparability, spatial scale and the diagnostic nature of the analytical framework.

First, the analysis used nationally consistent JAXA LULC data, which enabled comparison across provinces and time periods. However, all remotely sensed LULC products contain classification uncertainty. Confusion between spectrally or thematically similar classes may influence the transition matrices, annualized change rates, dominant transition pathways, and entropy-based indicators. This is particularly relevant where transitions occur between categories that are difficult to distinguish consistently, such as grass/shrubland, agriculture, bare land and some built-up or transitional surfaces. Aggregating the original classification into six broader LULC classes and conducting the analysis at a provincial scale likely reduces some pixel-level noise, but it does not remove classification error. In addition, this study did not include independent ground validation using field observations, high-resolution reference samples, or administrative land records. Future work should therefore compare the JAXA-derived transitions with independent LULC products, cadastral or land-administration datasets, or targeted validation samples to assess the sensitivity to classification uncertainty and to better understand the reliability of the results.

Second, entropy should be interpreted as a measure of transition diversity or pathway concentration, not as a complete measure of land-system complexity. In this study, Shannon entropy summarizes how total converted area is distributed across inter-category transition pathways. Lower entropy indicates that change is concentrated in fewer dominant transitions, whereas higher entropy indicates that change is distributed across a wider set of pathways. However, entropy does not identify which transitions are responsible for the observed patterns, nor does it capture the spatial arrangement, fragmentation, ecological quality, permanence, or socio-economic meaning of those transitions. Two provinces may therefore have similar entropy values but very different dominant pathways or governance implications. For this reason, the entropy analysis was interpreted alongside dominant transition analysis, maximum transition share, and spatial autocorrelation, rather than as a standalone measure of land-system complexity.

Third, temporal comparability between the two study periods requires careful interpretation. The 2000–2020 interval provides a long-term pre-2020 baseline, whereas the 2020–2023 interval represents the most recent period available at the time of analysis. To make these unequal periods comparable, all change magnitudes were expressed as annualized intensities, standardized by provincial area and interval duration. This avoids comparing a raw converted area over a 20-year period with a raw converted area over a three-year period. Nevertheless, the shorter 2020–2023 interval is inherently more sensitive to short-term fluctuations, classification uncertainty, temporary land cover states, and possible map-to-map inconsistencies. The post-2020 results should therefore be interpreted as evidence of recent change dynamics relative to the 2000–2023 baseline, rather than as confirmation of a persistent long-term trajectory. Additional years of consistent LULC data will be needed to determine whether the observed recent acceleration persists, stabilizes, or represents a short-term fluctuation.

Fourth, the regime typology is based on defined threshold criteria and should be understood as an analytical classification rather than a fixed categorization. Uncertainty may arise from the selection of threshold values used to distinguish accelerated, stable, concentrated, and diversified regimes, particularly for provinces located close to classification boundaries. Although sensitivity checks using nearby threshold values indicated that the main spatial patterns were generally stable, some provinces near the thresholds may change category under alternative threshold definitions. The typology should therefore be interpreted as a diagnostic tool for comparing provincial land-change profiles, not as a definitive classification of land governance status.

Fifth, we acknowledge that this study does not provide a comprehensive causal analysis of the underlying drivers of LULC change. The spatial autocorrelation analysis is diagnostic rather than explanatory. Moran's I and LISA are used to detect spatial dependence and identify local clusters of increased annualized land-change intensity, but they do not identify the causal mechanisms underlying these clusters. Although population density and administrative status are included as contextual indicators, land-change processes are shaped by a wider set of factors, including infrastructure development, industrial investment, agricultural policy, land use planning, accessibility, and biophysical constraints; however, these factors are not formally modeled here. Future research should combine the diagnostic framework developed in this study with spatial regression or other causal modeling frameworks to assess the drivers of provincial land-change regimes and explain why particular land-change regimes emerge in different provinces.

Finally, although the provincial scale aligns with land use planning administrative implementation in Vietnam, it may mask substantial intra-provincial variation. Provinces can contain diverse urban, agricultural, coastal, deltaic, and upland environments, and the same provincial-level regime may therefore include multiple local land-change processes.

Because Vietnam has an elongated north–south geographic configuration, province-level contiguity relationships are also spatially directional, which may influence the interpretation of Moran’s I clustering patterns. The spatial autocorrelation results should therefore be interpreted as indicative spatial tendencies and not as precise measures of directional spatial dependence.

Despite these limitations, the study provides a consistent and reproducible multidimensional diagnostic assessment of recent LULC change in Vietnam. By distinguishing annualized change rates, transition diversity, dominant pathways, and spatial clustering, the framework supports comparative analysis of provincial land-change regimes, while remaining open to further refinement with additional validation data, a longer time series, and explanatory driver modeling.

## 5. Conclusions

This study provided a multidimensional assessment of provincial LULC change in Vietnam, identifying a marked recent increase in annualized change rates during 2020–2023 relative to the 2000–2020 baseline, together with strong inter-provincial variation and spatial clustering.

Structural dynamics, measured by changes in entropy, indicate diverse trajectories across provinces. Some provinces experienced declining entropy and greater concentration in a limited number of transition pathways, while others showed more diversified transition portfolios. Importantly, only four of 34 provinces (11.8%) fell into the Accelerated–Concentrated category, whereas diversified regimes (Accelerated–Diversified and Stable–Diversified) accounted for about two-thirds of the provinces. These results indicate that higher annualized rates of change do not necessarily correspond to structural simplification.

The analysis of dominant transitions shows that land transformation is not driven by a single national pathway but by province-specific transition patterns, highlighting spatial variation in land-change processes. In addition, population density showed a moderate positive association with rates of conversion but remains weakly correlated with structural configuration, reinforcing the distinction between magnitude and compositional dynamics.

By combining intensity metrics, entropy-based structural measures, dominant transition analysis, and spatial clustering within a single framework, this study extends single-indicator approaches to land-change assessment. The proposed typology provides a reproducible analytical framework for comparing provincial land-change regimes, providing a diagnostic basis for identifying where differentiated land governance questions should be examined in more detail. The identified regime patterns may also support spatially differentiated land-management and regional planning strategies in rapidly transforming provinces. Future work could extend the current framework by incorporating variables such as infrastructure expansion, GDP or industrial investment, land use planning decisions, agricultural restructuring, elevation, accessibility, and policy implementation differences. Such an extension would allow the diagnostic regime typology developed here to be used for more detailed explanatory modelling.

**Supplementary Materials:** The following supporting information can be downloaded at: <https://www.mdpi.com/article/10.3390/land15061040/s1>, including a description of LULC data and preprocessing, LULC classification scheme, LULC maps for 2000, 2020, and 2023 (Figure S1), LULC transition matrices for 2000–2020 and 2020–2023, the provincial analytical dataset, and spatial autocorrelation results. References [33,40] are cited in the Supplementary Materials.

**Author Contributions:** Conceptualization, A.T.N. and L.S.; methodology, A.T.N. and L.S.; formal analysis, A.T.N.; investigation, A.T.N.; data curation, A.T.N.; writing—original draft preparation, A.T.N. and L.S.; writing—review and editing, A.T.N. and L.S.; visualization, A.T.N. All authors have read and agreed to the published version of the manuscript.

**Funding:** This research received no external funding.

**Data Availability Statement:** The data used in this study are publicly available. The land use and land cover (LULC) datasets were obtained from the Japan Aerospace Exploration Agency (JAXA) and can be accessed at [https://www.eorc.jaxa.jp/ALOS/en/dataset/lulc\\_e.htm](https://www.eorc.jaxa.jp/ALOS/en/dataset/lulc_e.htm) (accessed on 21 January 2026). Derived data supporting the findings of this study are available from the corresponding author upon reasonable request.

**Acknowledgments:** The data used in this study were provided by the Japan Aerospace Exploration Agency (JAXA). ChatGPT v4.5 (OpenAI) was used for language editing. The authors take full responsibility for the content.

**Conflicts of Interest:** The authors declare no conflicts of interest.

## Abbreviations

The following abbreviations are used in this manuscript:

LULC	Land use and land cover
LISA	Local indicators of spatial association
JAXA	Japan Aerospace Exploration Agency
MONRE	Ministry of Natural Resources and Environment (Vietnam)
P1	Study period 1 (2000–2020)
P2	Study period 2 (2020–2023)
$\Delta S$	Change in intensity ( $S_{P2} - S_{P1}$ )
$\Delta H$	Change in Shannon entropy

## References

1. Turner, B.L.; Lambin, E.F.; Reenberg, A. The emergence of land change science for global environmental change and sustainability. *Proc. Natl. Acad. Sci. USA* **2007**, *104*, 20666–20671. [[CrossRef](#)] [[PubMed](#)]
2. Seto, K.C.; Güneralp, B.; Hutyrta, L.R. Global forecasts of urban expansion to 2030 and direct impacts on biodiversity and carbon pools. *Proc. Natl. Acad. Sci. USA* **2012**, *109*, 16083–16088. [[CrossRef](#)]
3. Zhao, Q.; Yu, L.; Chen, X. Land system science and its contributions to sustainable development goals: A systematic review. *Land Use Policy* **2024**, *143*, 107221. [[CrossRef](#)]
4. Liu, J.; Daily, G.C.; Ehrlich, P.R.; Luck, G.W. Effects of household dynamics on resource consumption and biodiversity. *Nature* **2003**, *421*, 530–533. [[CrossRef](#)]
5. Güneralp, B.; Reba, M.; Hales, B.U.; Wentz, E.A.; Seto, K.C. Trends in urban land expansion, density, and land transitions from 1970 to 2010: A global synthesis. *Environ. Res. Lett.* **2020**, *15*, 044015. [[CrossRef](#)]
6. United Nations. *World Urbanization Prospects 2025: Summary of Results*; United Nations: New York, NY, USA, 2025; p. 109.
7. Lwasa, S.; Seto, K.C.; Bai, X.; Blanco, H.; Gurney, K.R.; Kilkis, Ş.; Lucon, O.; Murakami, J.; Pan, J.; Sharifi, A.; et al. Urban systems and other settlements. In *Climate Change 2022: Mitigation of Climate Change*; Intergovernmental Panel on Climate Change (IPCC): Geneva, Switzerland, 2022. [[CrossRef](#)]
8. Seto, K.C.; Fragkias, M. Quantifying Spatiotemporal Patterns of Urban Land use Change in Four Cities of China with Time Series Landscape Metrics. *Landsc. Ecol.* **2005**, *20*, 871–888. [[CrossRef](#)]
9. Wu, J.; Luo, J.; Zhang, H.; Yu, M. Driving forces behind the spatiotemporal heterogeneity of land use and land cover change: A case study of the Weihe River Basin, China. *J. Arid Land* **2023**, *15*, 253–273. [[CrossRef](#)]
10. Su, D.; Yang, K.; Peng, Z.; Sun, R.; Zhang, M.; Ma, L.; Ma, J.; Li, T. Analysing the Spatial and Temporal Characteristics of Ecological Land Encroachment by Cropland Expansion and Its Drivers in Cambodia. *Land* **2024**, *13*, 2195. [[CrossRef](#)]
11. Zhang, M.; Ning, L.; Li, J.; Wang, Y. Study on Spatial Pattern Changes and Driving Factors of Land Use/Cover in Coastal Areas of Eastern China from 2000 to 2022: A Case Study of Jiangsu Province. *Land* **2025**, *14*, 2031. [[CrossRef](#)]
12. Zhai, D.; Zhang, X.; Zhuo, J.; Mao, Y. Driving the Evolution of Land Use Patterns: The Impact of Urban Agglomeration Construction Land in the Yangtze River Delta, China. *Land* **2024**, *13*, 1514. [[CrossRef](#)]

13. Pontius, R.G.; Shusas, E.; McEachern, M. Detecting important categorical land changes while accounting for persistence. *Agric. Ecosyst. Environ.* **2004**, *101*, 251–268. [[CrossRef](#)]
14. Aldwaik, S.Z.; Pontius, R.G. Intensity analysis to unify measurements of size and stationarity of land changes by interval, category, and transition. *Landsc. Urban Plan.* **2012**, *106*, 103–114. [[CrossRef](#)]
15. Huang, J.; Pontius, R.G.; Li, Q.; Zhang, Y. Use of intensity analysis to link patterns with processes of land change from 1986 to 2007 in a coastal watershed of southeast China. *Appl. Geogr.* **2012**, *34*, 371–384. [[CrossRef](#)]
16. Shannon, C.E. A Mathematical Theory of Communication. *Bell Syst. Tech. J.* **1948**, *27*, 379–423. [[CrossRef](#)]
17. Herold, M.; Couclelis, H.; Clarke, K.C. The role of spatial metrics in the analysis and modeling of urban land use change. *Comput. Environ. Urban Syst.* **2005**, *29*, 369–399. [[CrossRef](#)]
18. Kudas, D.; Wnęk, A.; Hudecová, L.; Fencik, R. Spatial Diversity Changes in Land Use and Land Cover Mix in Central European Capitals and Their Commuting Zones from 2006 to 2018. *Sustainability* **2024**, *16*, 2224. [[CrossRef](#)]
19. Moran, P.A.P. Notes on continuous stochastic phenomena. *Biometrika* **1950**, *37*, 17–23. [[CrossRef](#)]
20. Anselin, L. Local Indicators of Spatial Association—LISA. *Geogr. Anal.* **1995**, *27*, 93–115. [[CrossRef](#)]
21. Tang, X.; Xu, J.; Wang, R.; Li, J.V.; Jiang, L.; Li, C.Z. Drivers of Cross-Boundary Land Use and Cover Change in a Megacity Region: Evidence from the Guangdong–Hong Kong–Macao Greater Bay Area. *Sustainability* **2026**, *18*, 470. [[CrossRef](#)]
22. Retamoza-González, E.A.; Eaton-González, B.R.; Leyva-Aguilera, J.C.; Reyes-Orta, M.; Arias-Rojo, H.M. Identifying priority restoration areas by mapping land use change drivers. *Environ. Chall.* **2026**, *22*, 101399. [[CrossRef](#)]
23. Song, X.; Chen, F.; Sun, Y.; Ma, J.; Yang, Y.; Shi, G. Effects of land utilization transformation on ecosystem services in urban agglomeration on the northern slope of the Tianshan Mountains, China. *Ecol. Indic.* **2024**, *162*, 112046. [[CrossRef](#)]
24. Kontgis, C.; Schneider, A.; Fox, J.; Saksena, S.; Spencer, J.H.; Castrence, M. Monitoring peri-urbanization in the greater Ho Chi Minh City metropolitan area. *Appl. Geogr.* **2014**, *53*, 377–388. [[CrossRef](#)]
25. Tuan, N.T. Urbanization and land use change: A study in Vietnam. *Environ. Socio-Econ. Stud.* **2022**, *10*, 19–29. [[CrossRef](#)]
26. World Bank Group. *Vietnam's Urbanization at a Crossroads: Embarking on an Efficient, Inclusive, and Resilient Pathway (Overview)*; World Bank: Washington, DC, USA, 2020. [[CrossRef](#)]
27. Phan, D.C.; Trung, T.H.; Truong, V.T.; Sasagawa, T.; Vu, T.P.T.; Bui, D.T.; Hayashi, M.; Tadono, T.; Nasahara, K.N. First comprehensive quantification of annual land use/cover from 1990 to 2020 across mainland Vietnam. *Sci. Rep.* **2021**, *11*, 9979. [[CrossRef](#)]
28. Guo, X.; Ye, J.; Hu, Y. Analysis of Land Use Change and Driving Mechanisms in Vietnam during the Period 2000–2020. *Remote Sens.* **2022**, *14*, 1600. [[CrossRef](#)]
29. Disperati, L.; Virdis, S.G.P. Assessment of land use and land cover changes from 1965 to 2014 in Tam Giang-Cau Hai Lagoon, central Vietnam. *Appl. Geogr.* **2015**, *58*, 48–64. [[CrossRef](#)]
30. Schaefer, M.; Thinh, N.X. Evaluation of Land Cover Change and Agricultural Protection Sites: A GIS and Remote Sensing Approach for Ho Chi Minh City, Vietnam. *Heliyon* **2019**, *5*, e01773. [[CrossRef](#)] [[PubMed](#)]
31. Vu, T.-T.; Shen, Y. Land use and Land cover Changes in Dong Trieu District, Vietnam, during Past Two Decades and Their Driving Forces. *Land* **2021**, *10*, 798. [[CrossRef](#)]
32. Bui, D.H.; Mucsi, L. Land use change and urban expansion in Binh Duong province, Vietnam, from 1995 to 2020. *Geocarto Int.* **2022**, *37*, 17096–17118. [[CrossRef](#)]
33. Japan Aerospace Exploration Agency (JAXA). *High-Resolution Land Use and Land Cover Map (HRLULC), version 25.09*; Japan Aerospace Exploration Agency (JAXA): Ibaraki, Japan, 2026. Available online: [https://www.eorc.jaxa.jp/ALOS/en/dataset/lulc\\_e.htm](https://www.eorc.jaxa.jp/ALOS/en/dataset/lulc_e.htm) (accessed on 21 February 2026).
34. Ministry of Natural Resources and Environment (MONRE). QCVN 78:2023/BTNMT: National Technical Regulation on Establishment of Land Cover Datasets for Greenhouse Gas Emission Calculation Using Optical Remote Sensing Data. Vietnam Government Portal, Hanoi, Vietnam. Available online: <https://datafiles.chinhphu.vn/cpp/files/vbpq/2024/01/25-btnmt-kem.pdf> (accessed on 15 March 2026).
35. Fan, Y.; Yu, G.; He, Z.; Yu, H.; Bai, R.; Yang, L.; Wu, D. Entropies of the Chinese Land Use/Cover Change from 1990 to 2010 at a County Level. *Entropy* **2017**, *19*, 51. [[CrossRef](#)]
36. Liu, J.; Hu, Y.; Feng, Z.; Xiao, C. A Review of Land Use and Land Cover in Mainland Southeast Asia over Three Decades (1990–2023). *Land* **2025**, *14*, 828. [[CrossRef](#)]
37. Meyfroidt, P.; Lambin, E.F. Global Forest Transition: Prospects for an End to Deforestation. *Annu. Rev. Environ. Resour.* **2011**, *36*, 343–371. [[CrossRef](#)]
38. Liu, X.; Li, X.; Chen, Y.; Tan, Z.; Li, S.; Ai, B. A new landscape index for quantifying urban expansion using multi-temporal remotely sensed data. *Landsc. Ecol.* **2010**, *25*, 671–682. [[CrossRef](#)]

39. Güneralp, B.; Ahasan, R. Urban land-change futures: Current understanding, challenges, and implications. *npj Urban Sustain.* **2025**, *6*, 7. [[CrossRef](#)]
40. Japan Aerospace Exploration Agency (JAXA). *Vietnam-Wide 30-m Annual Land-Use Land-Cover Data Sets (VLUCDs), Version 23.09*; Japan Aerospace Exploration Agency (JAXA): Ibaraki, Japan, 2023.

**Disclaimer/Publisher's Note:** The statements, opinions and data contained in all publications are solely those of the individual author(s) and contributor(s) and not of MDPI and/or the editor(s). MDPI and/or the editor(s) disclaim responsibility for any injury to people or property resulting from any ideas, methods, instructions or products referred to in the content.